ORIGINAL PAPER

Tuning structure and morphology of sheath-core bicomponent polyolefin fibres modified by grafting of vinylbenzyl chloride in emulsion and solvent media

Teo Ming Ting[1*], Ebrahim Abouzari Lotf[2,3], Mohamed Mahmoud Nasef[3,4*], Wen Soong Lok[1], Thye Foo Choo[1], Nur Athilah Kamarudin[1], Ee Ling Aw[1], Nur Ashikin Mohamed[3]

[1]Radiation Processing Technology Division, Malaysian Nuclear Agency, 43000, Kajang, Selangor, Malaysia
[2]Trinseo Deutschland Anlagengesellschaft mbH, Industriestraße 1, 77836 Rheinmünster, Germany
[3]Center of Hydrogen Energy, Institute of Future Energy, Universiti Teknologi Malaysia, 54100, Kuala Lumpur, Malaysia
[4]Department of Chemical and Environmental Engineering, Malaysia Japan International Institute of Technology, Universiti Teknologi Malaysia, 54100, Kuala Lumpur, Malaysia

[*]*Correspondence:* Teo Ming Ting (tmting@nm.gov.my); Mohamed Mahmoud Nasef (mahmoudeithar@cheme.utm.my)

Received: 4 December 2025, Revised: 4 February 2026, Accepted: 9 February 2026
DOI: **10.22063/POJ.2026.35813.1380**

ABSTRACT

Bicomponent polyethylene (PE)/polypropylene (PP) non-woven sheets made from sheath-core fibres were modified by radiation-induced grafting (RIG) of vinylbenzyl chloride (VBC) monomer in both emulsion- and solvent-mediated systems under varying conditions. The key grafting parameters, including reaction medium, monomer concentration, absorbed dose, and temperature, were systematically investigated to control the grafting yield (GY%) and its distribution across fibres. The structural, morphological, and chemical properties of the resulting poly(VBC) grafted fibres were evaluated using Fourier transform infrared spectroscopy (FTIR), field emission scanning electron microscopy (FESEM) coupled with energy-dispersive X-ray spectroscopy (EDX), elemental analysis, X-ray diffraction (XRD), thermogravimetric analysis (TGA), differential scanning calorimetry (DSC), and contact angle measurements. The results demonstrated that the reaction medium significantly influenced both the grafting yield (GY%) and graft distribution. Diffusion of poly(VBC) occurred similarly across the sheath and core; however, distinct differences in grafting rates and yields were observed between the emulsion and solvent systems. Under emulsion conditions, a higher density of poly(VBC) grafts was incorporated into the PE sheath than into the PP core compared to solvent-mediated grafting, whereas the side-chain grafts exhibited a generally homogeneous distribution throughout the bicomponent fibres in both systems. These findings demonstrate an effective approach for tuning the structure and morphology of PE/PP bicomponent fibres, favouring the emulsion system, offering valuable insights for the design of advanced functional materials with promising applications in environmental remediation and electrochemical energy systems.

Keywords: Sheath-core bicomponent polyethylene/polypropylene fibres; radiation-induced grafting; vinylbenzyl chloride; effect of grafting medium; precursor for functional graft copolymers.

Highlights

- Radiation grafting of VBC allowed tuning PE/PP fibre composition and morphology
- Graft yield is function of monomer concentration, radiation dose and temperature
- Reaction medium notably affected grafting yield and distribution across fibres
- Emulsion achieved higher graft yields than solvent under similar conditions
- Grafted fibres showed integrity and suitability for energy/environmental uses

INTRODUCTION

Synthetic polymer fibres with bicomponent sheath-core structures are receiving increasing attention due to their versatile properties, such as improved strength, flexibility, durability and chemical resistance. These properties originate from integrating two different polymers arranged in a sheath-core structure, making them suitable for a wide range of applications. Generally, the core layer primarily gives the desired mechanical strength, dimensional and thermal stability, and the sheath layer provides functionality for specific applications [1]. This combined structure is fabricated by extruding two polymers through a single spinneret, where polyethylene (PE) is frequently used as the sheath layer, with polypropylene (PP), polyamide 6 (PA6), or polyester used as the core [1,2]. The polymer used as the core usually has higher elastic modulus values than the sheath polymer, and the cross-sectional area of the core is always larger than that of the sheath. Due to the desired melting behaviour and elasticity modulus, PE/PP fibres are the preferred choice for critical components in many applications, such as flame retardancy, insulation, medical products, diapers, sanitary napkins, filtration materials, and geotextiles [1,3,4]. Furthermore, electrical conductivity was enhanced by incorporating bicomponent PE/PP fibres into nonwoven fabrics compared to counterparts made of parent polymers (PE and PP) [5]. Also, tensile strength and alkaline resistance were found to be improved by using bicomponent PE/PP fibres as separators in alkaline batteries compared to those made from single-component PE or PP fibres [4]. During the fabrication of fabric made from PE/PP fibres, thermal bonding is used to combine the two polymers, i.e. the fabric is heated to a temperature sufficient to soften PE component, while PP component remains solid. Upon cooling, the molten PE solidifies and bonds the fibres together, providing structural integrity to the fabric. Hence, there are thermally bonded points in bicomponent PE/PP fabrics that can undergo large deformations during uniaxial tensile loading before fracturing, caused by the interlocking structure created by the melted and solidified polymers [6].

The excellent properties of these bicomponent materials and their inherent low cost have resulted in growing interest from research and industrial perspectives. However, the properties of the polymeric materials need to be modified for specific applications. Desired functionality could be introduced to PE/PP fibres by graft copolymerization methods, such as chemical treatment [7], photografting with UV, plasma polymerisation, and ionising radiation treatment [8]. These treatments can be used to

improve surface wettability [9], introduce ionic moieties [10], and create binding sites for metals [8] and other elements [11–12]. Radiation-induced grafting (RIG) is a widely applied technique for fibre modification due to its effectiveness, operational simplicity, and ability to control the grafting levels precisely. RIG can be carried out in aqueous or organic solvent systems as well as in emulsion media.

Although comparable grafting yields and uniform graft distributions at the macroscopic scale can be achieved using both solvent- and emulsion-mediated approaches, but the microscopic counterpart may differ. Nevertheless, emulsion-mediated RIG has a more environmentally benign nature as water replaces hazardous organic solvents and offers superior efficiency by requiring lower monomer consumption, reducing irradiation doses, and allowing for initiation at ambient temperature, thereby enhancing the overall cost-effectiveness and sustainability of the grafting process [8].

Various bicomponent polymers of PE/PP, PE/polyester, and PE/nylon substrates have been functionalised with diverse monomers such as acrylic acid, glycidyl methacrylate (GMA), methyl methacrylate, dimethyl aminoethyl methacrylate, methacrylic acid, and acrylonitrile using RIG [8, 13–15]. However, grafting behaviour was not investigated with respect to the location of grafting, i.e., on the sheath or the core. Earlier, studies on grafting location reports were limited to porous polymer films. For example, GMA onto porous PE film revealed that poly(GMA) chains preferentially extend from the pore surfaces toward the pore interior, with polymer roots penetrating the polymer matrix [16]. On the other hand, RIGC of N-vinylformamide (NVFM) onto ultrahigh molecular weight polyethylene (UHMWPE) porous films showed that poly(NVFM) grafts predominantly grow from the pore walls and propagate toward the centre of the pores, where opposing graft chains either meet or terminate due to monomer depletion [17]. These studies highlight that grafting location and propagation pathways are governed by a complex interplay of monomer diffusion, substrate porosity, and polymer–monomer interactions. However, such investigations have been largely limited to homogeneous or porous polyethylene substrates, and the grafting behaviour in structurally heterogeneous systems, such as sheath–core bicomponent fibres, remains insufficiently explored.

Vinylbenzyl chloride (VBC), also known as chloromethylbenzene, is a versatile monomer with dual functionality that exhibits high reactivity. The benzylic chlorine atom readily undergoes nucleophilic substitution reactions, enabling diverse chemical modification. Concurrently, the vinyl group provides an active site for polymerisation or copolymerization under relatively mild conditions with a variety of initiators [18]. VBC has often been employed to prepare precursors for functional copolymers by grafting onto polymer fibres and sheets. This strategy enables the generation of a diverse range of functional materials, which can subsequently undergo post-grafting modifications to yield products such as adsorbents and polymer electrolyte membranes for applications in environmental and renewable energy technologies [19–28].

To our knowledge, there is no clear evidence whether grafting is taking place on one or both components of sheath-core fibres. Fundamentally, the monomer accessibility to the different components of bicomponent fibres is influenced by diffusion, which is a function of swelling,

hydrophilicity, crytallinity, and porosity, all of which can be varied by manipulation of grafting parameters. Therefore, it is highly significant to understand the grafting location to determine the suitability of grafted bicomponent fabrics for applications such as adsorbents and battery separators.

The present study aims to explore the tunability of the structure and morphology of bicomponent sheath–core PE/PP fibres in the form of nonwoven sheets, through RIG of VBC using both emulsion- and solvent-mediated systems under varying reaction conditions. The fibres' physical, chemical, and thermal properties were systematically characterised using a suite of analytical techniques. Particular emphasis was placed on assessing the distribution of poly(VBC) side chains across the sheath–core structure, to elucidate the correlation between reaction parameters, grafting yield, and structural changes uniformity.

EXPERIMENTAL

Materials

VBC (mixture of *meta*- and *para*-isomers, 97% purity) and polyoxyethylenesorbitan monolaurate (Tween-20) were supplied by Sigma-Aldrich. The monomer was used as received without any purification. PE/PP non-woven sheet with an areal weight of 70 ± 10% g/m^2, was provided by Kurashiki Co. Methanol and propanol were research grade and purchased from Fisher Scientific. Double-distilled (DD) water was used as a solvent in emulsion-mediated RIG.

Grafting of VBC onto nonwoven fabric

PE/PP nonwoven sheets were cleaned, vacuum-dried, and cut into 2 × 3 cm pieces, followed by weighing. Each sample was sealed in a nitrogen-purged PE bag and irradiated using an electron beam accelerator (NHV-Nissin High Voltage, EPS 3000) operated at 2 MeV and 2.0 mA. Sample irradiation was performed on dry ice with a total dose of 50–300 kGy at 25 kGy per pass. The irradiated samples were transferred to evacuated glass ampoules for grafting reactions. For emulsion grafting, a solution of VBC and Tween-20 (polyoxyethylene sorbitan monolaurate) in DD water was prepared, while for solvent grafting, VBC was diluted with methanol to the desired concentration. The grafting solutions were purged with nitrogen for 30 min before being used in the reaction. The solutions were then introduced into the ampoules containing the irradiated samples via vacuum stopcock, after which the ampoules were sealed and heated in a thermostatic water bath at 40–70 °C for planned periods ranging from 2 to 180 min. VBC concentration was varied from 1–20 wt%. Following the reaction, the grafted substrates were washed repeatedly with propanol and vacuum-dried at 40 °C for 12 h.

The grafting yield (*GY*) was determined gravimetrically from weight increase after grafting according to equation (1) and further confirmed by elemental analysis.

$$GY\,(\%) = \frac{W_g - W_s}{W_s} \times 100 \qquad (1)$$

where W_s and W_g are the weights of the nonwoven sheet sample before and after grafting, respectively.

Characterisation and measurements

The composition of the grafted samples was investigated by Fourier Transform infra-red (FTIR) spectroscopy (Bruker Tension II FTIR spectrometer) fitted with attenuated total reflectance (ATR). To further evaluate the composition of the grafted substrates, samples were fractured after dipping in liquid nitrogen, and the composition profile was achieved by Energy Dispersive X-ray spectroscopy (EDS) with a detector energy resolution of 135-150 eV using Zeiss GeminiSEM 500. The morphology of the samples was studied using a GEMINI500 (Germany) field emission scanning electron microscopy (FESEM) by which both surface and cross-sections of samples were sputter-coated with platinum using an Auto-fine coater (JEC-3000FC, JEOL, Japan) for 30 s at 20 mA. X-Ray Diffraction (XRD) of the samples was investigated with X'pert Pro X-ray diffractometer of PW 3040, Philips, (λ = 0.15406 nm) at 45 kV and 20 mA in a diffraction angle range of 10-80˚ with a scanning rate of 2˚ min^{-1}. A LECO CHNS-932 elemental analyser was used to confirm the grafting and obtain the elemental composition of substrates. Thermal properties of the samples were investigated using a Mettler-Toledo, DSC1 calorimeter with a heating rate of 10 ˚C min^{-1} under N_2 atmosphere. Thermal stability of the samples was determined using thermogravimetric analysis (TGA), and the measurement was performed on a Perkin Elmer, TGA-Pyris 1 at a heating rate of 10 ˚C min^{-1} under N_2 atmosphere. Contact angle measurements of a liquid on the surface of the pristine and grafted PE/PP sheets were carried out using a Biolin Scientific Attension® Theta optical contact angle analyser. Three different measurements were performed for each sample, and an average reading was recorded.

RESULTS AND DISCUSSION

Effect of irradiation dose

Figure 1 illustrates the effect of absorbed dose on GY% in emulsion- (Figure 1a) and solvent-mediated (Figure 1b) grafting systems at various reaction times. In both systems, GY% generally increased with the absorbed dose from 50 to 300 kGy, as higher doses generate more radicals on the polymer substrate, leading to greater initiation sites, more grafted growing chains, and consequently higher GY%. The emulsion system consistently exhibited higher GY% (than the solvent system at similar absorbed doses and reaction times). Furthermore, for most constant absorbed doses, GY% increases with time, indicating that the chains were likely grown in length with time.

A similar trend, i.e. grafting in an emulsion system had higher GY% vs. grafting in a solvent system, was also observed for the emulsion RIG of acrylic acid onto PE fabric [14], methacrylic acid, acrylamide, and dimethyl acrylamide onto PE powder [29], glycidyl methacrylate (GMA) onto PE/PP [30] and VBC onto nylon-6 fibres [27]. Unlikely, the grafting of styrene diluted with methanol onto PP fibres showed a low increasing trend in GY% reaching a maximum of 18% with the dose rise from 8 to 200 kGy, and this implied the addition of grafting enhancers, such as sulfuric acid and polyfunctional monomer, to reach higher GY (80%) [31]. On the other hand, grafting of GMA diluted with methanol and grafted onto porous PE films reported by Saito and coworkers (16) demonstrated that GY% increased with increasing absorbed dose, indicating enhanced radical generation. Grafting behaviour

was found to be strongly governed by irradiation dose and accompanied by monomer diffusion within the pore network. Graft initiation occurred at the pore walls, followed by propagation toward the pore interior, with polymer roots invading PE matrix.

In the emulsion system (Figure 1a), GY% rose sharply up to 30 min, then slowed yet remained increasing at 120–180 min. In contrast, the solvent-mediated grafting system (Figure 1b) showed a gradual increase from 2 to 120 min before slowing down to almost reaching saturation, before increasing again with further dose rise. This behaviour is due to progressive formation of radicals up to 120 min, then slowed down likely due to radical recombination, coinciding with the high chain transfer coefficient of menthol (solvent). At higher doses, grafting increased sharply again, likely due to chain scission and the generation of new radicals that promoted further grafting. Overall, these results confirm that GY% is dose-dependent in both systems, with the emulsion-mediated process achieving superior grafting efficiency.

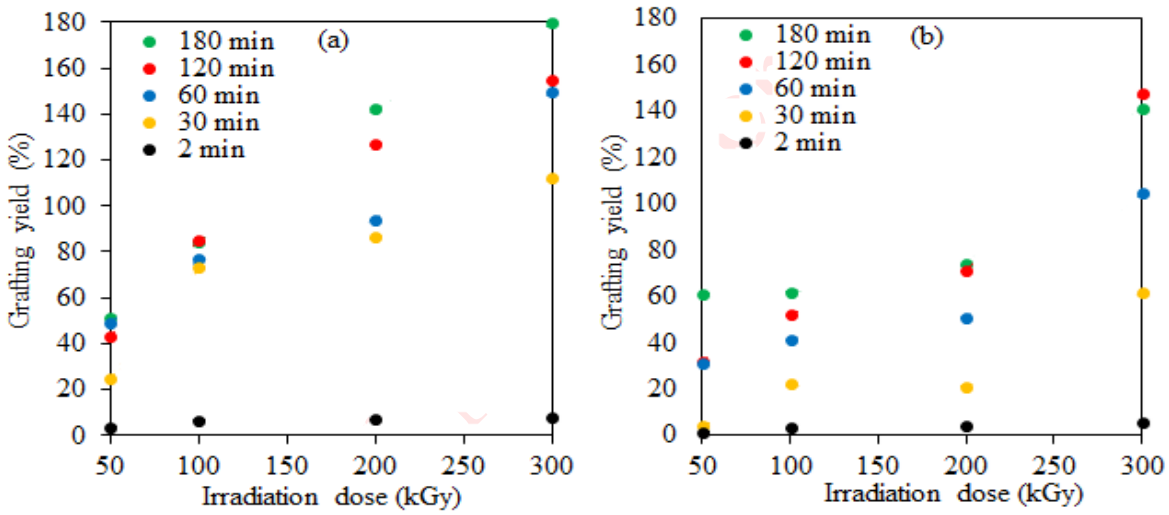

Figure 1. Variation of grafting yield with absorbed doses at various grafting times in: (a) emulsion mediated grafting (aqueous emulsion at 50 °C with monomer conc. of 5 wt% and Tween 20 conc. of 0.5 wt%) and (b) solvent-mediated grafting (methanol solvent at 60 °C and monomer conc. of 10 wt%).

Effect of monomer concentration

Figure 2 illustrates the variation in GY% with monomer concentration at different reaction times for emulsion-mediated (Figure 2a) and solvent-mediated (Figure 2b) grafting systems. In the emulsion-mediated grafting system (Figure 2a) for all reaction times except 2 min, GY% increased steadily as the VBC concentration increased from 1 to 10 wt%, beyond which it levelled off. No significant grafting was observed at 2 min across all the investigated concentrations.

For the solvent-mediated system (Figure 2b), the GY% increased gradually with both VBC concentration and reaction time, reaching a maximum value at 120 min before levelling off between 120 and 180 min. In the meantime, the GY% increased with monomer concentration up to 5% in

methanol, then plateaued before rising sharply again with further increase in the monomer concentration. The GY%-time behaviour is attributed to the enhanced rate of monomer diffusion and its abundance up to 120 min, after which grafting reached saturation because of the medium viscosity rise with homopolymerization and lack of monomer molecules close to the remaining radicals' vicinity. The GY%-monomer concentration behaviour can be attributed to an initial increase in GY% with monomer concentration due to greater monomer availability, plateaued when radicals are barred by viscosity rise and competing homopolymers accumulation and then rises again at high concentrations, where enhanced diffusion changes reaction kinetics, allowing more access to radicals, favouring grafting. The overall increase in GY% with both monomer concentration and reaction time is ascribed to the greater number of monomer molecules diffusing into active sites, thereby facilitating initiation and graft growing chain propagation.

Although the emulsion-mediated system requires lower monomer concentration, absorbed dose (100 kGy) and temperature (50 °C) compared with the solvent-mediated system (200 kGy, 60 °C), emulsion system achieved higher GY% values at monomer concentrations of 1, 5, and 10 wt%. At 20 wt%, however, both grafting systems exhibited comparable GY%. These results confirm the presence of higher grafting efficiency of the emulsion system, which enhances monomer accessibility to active grafting sites. Such a significant dependence of the GY% on the monomer concentration was reported earlier in the grafting of GMA or dimethyl aminoethyl methacrylate onto PE/PP [13], 4-vinylpyridine onto PE/PP and VBC onto both nylon-6 fibres [27] and poly(hexafluoropropylene-*co*-tetrafluoroethylene) film [23]. These results suggest that dependence of GY on absorbed dose and monomer concentration, highlighting the critical role of radical density and monomer availability in determining grafting efficiency

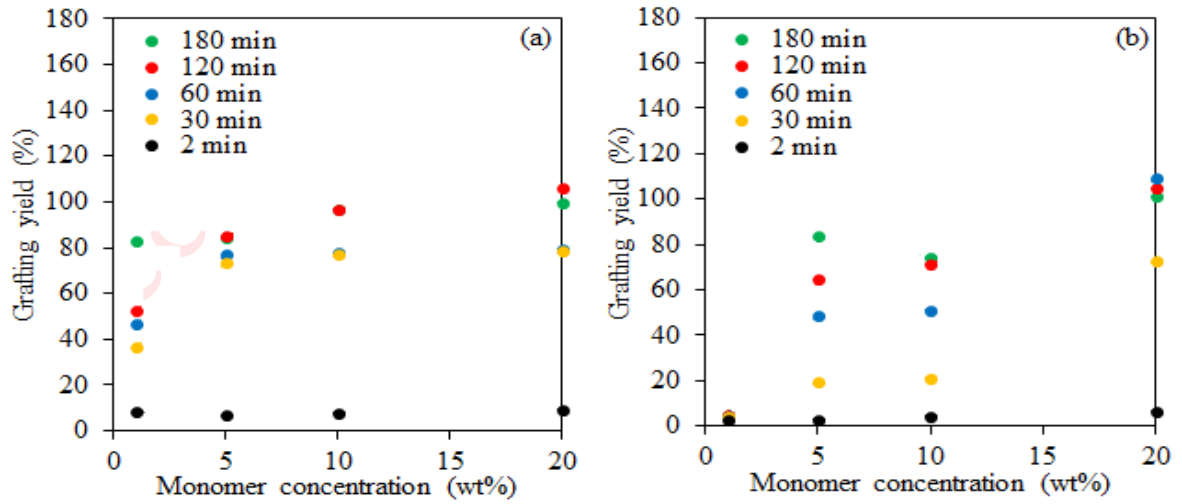

Figure 2. Variation of grafting yield with monomer concentrations at various grafting times in: (a) emulsion mediated grafting (aqueous emulsion at 50 °C, Tween-20 conc. of 0.5 wt% and absorbed dose of 100 kGy) and (b) solvent-mediated grafting (methanol solvent at 60 °C and absorbed dose of 200 kGy).

Effect of temperature

Figure 3 presents the effect of temperature on GY% at different reaction times for emulsion- (Figure 3a) and solvent-mediated (Figure 3b) grafting systems. In both cases, GY% increased with the temperature rise, which can be attributed to the combined effect of higher radical initiation rates and enhanced monomer diffusion into the grafting zone. These factors accelerate initiation and chain propagation, thereby increasing grafting efficiency. The emulsion grafting system displayed a pronounced rise in GY% between 2 and 30 min, whereas the solvent-mediated counterpart exhibited a gradual increase from 2 to 120 min. Beyond 120 min, the grafting yield reached a plateau in both systems, achieving grafting saturation. This behaviour is most likely attributed to mutual recombination of trapped radicals, which reduces the number of available monomer molecules and promotes chain termination. Notably, although the irradiation dose and monomer concentration employed in the emulsion grafting system were only half those used in the solvent system, the emulsion grafting still achieved a higher GY%. The grafting behaviour reported in the literature also agreed with the present study. For example, the grafting of GMA onto PE film [32], dimethylaminoethyl methacrylate onto PE/PP polymer [13], and the grafting of VBC onto nylon-6 fibres [27]. The RIG of VBC onto poly(hexafluoropropylene-*co*-tetrafluoroethylene) film showed a maximum GY% at 50 °C and started to decrease beyond 50 °C [23]. These results suggest that temperature control is highly essential for optimisation of grafting efficiency, and the emulsion grafting system is more temperature-responsive than solvent-mediated counterparts. Thus, it is more efficient for achieving higher GY% under lower monomer concentrations and absorbed doses.

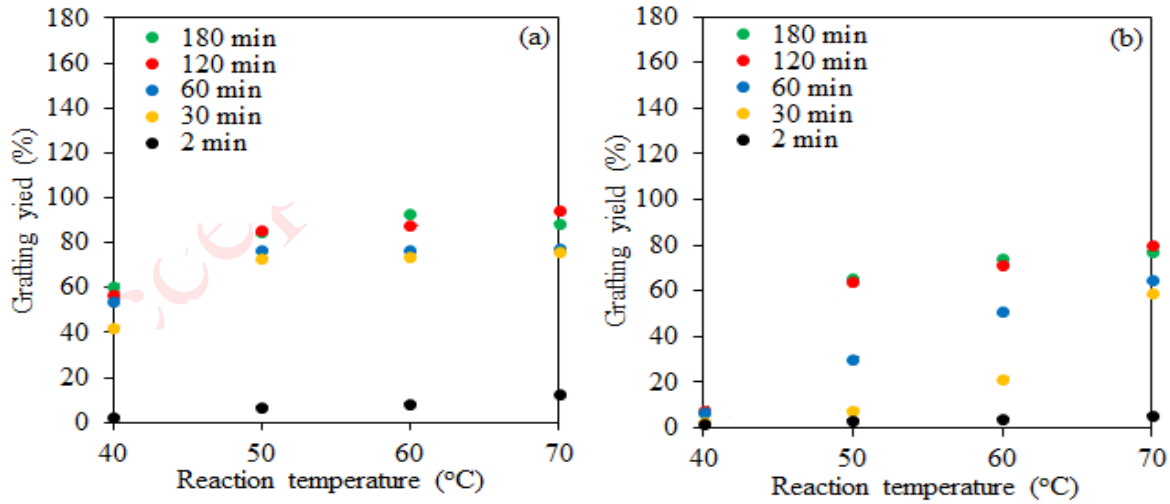

Figure 3. Variation of grafting yield with temperature at various grafting times in: (a) emulsion mediated (aqueous emulsion with monomer conc. of 5 wt% and Tween-20 of 0.5 wt%, with absorbed dose of 100 kGy) and (b) solvent-mediated (methanol solvent and monomer conc. of 10 wt% with absorbed dose of 200 kGy).

Chemical changes

Introducing poly(VBC) onto bicomponent PE/PP fibres was confirmed with FTIR spectroscopy. Figure 4 shows the spectra for original and grafted PE/PP with various GY%. The original PE/PP fibres exhibited PE-related characteristic peaks, such as CH_2 bending vibration at 1475 cm^{-1} and CH_2 rocking at 720 cm^{-1}. On the other hand, PP is marked by CH_3 bending vibration at roughly 1455 and 1375 cm^{-1}, and skeletal vibrations in the fingerprint region from 1175 to 998 cm^{-1}. The presence of these peaks confirms that both PE and PP are in the bicomponent fibres. Upon grafting, two strong bands appeared at 675 and 711 $cm^{-1,}$ corresponding to the CH bending of the 1,3-disubstituted benzene ring coupled with newly emerged peaks at 797-840 cm^{-1} representing aromatic C-H bonds of *para*-substitution. The intensity of these peaks was increased as the DG% increased from 40% to 150%. More importantly, the stretching vibration peak of C-Cl resembles the chloromethyl group at 1263 cm^{-1} of poly(VBC). The FTIR features of grafted samples confirm the successful grafting of VBC onto PE/PP fibres regardless of the medium of grafting.

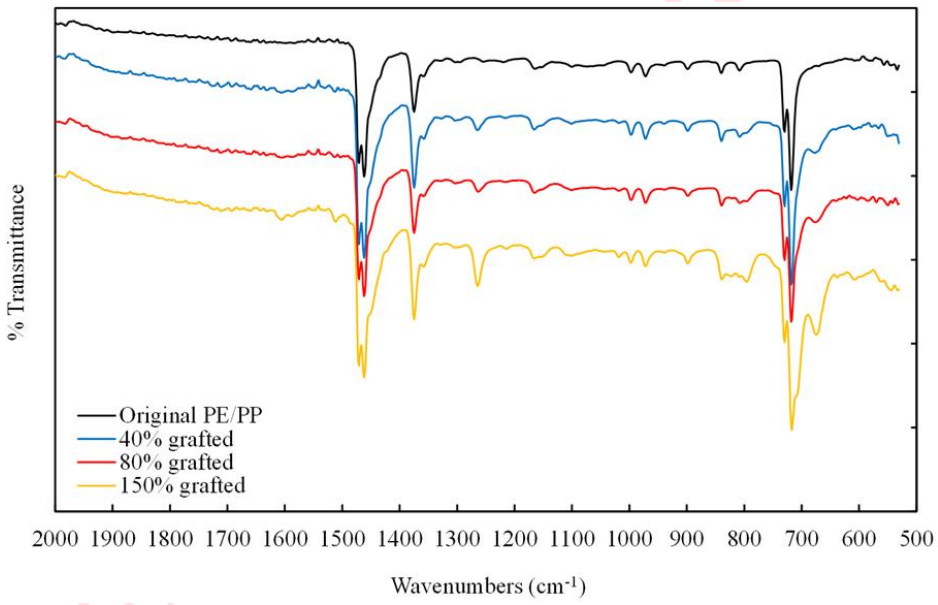

Figure 4. FTIR spectra of original PE/PP and poly(VBC) grafted fibres with various GY%.

FTIR analysis confirmed the incorporation of poly(VBC) onto the bicomponent PE/PP fibrous sheet by RIG as represented schematically in the plausible mechanism displayed in Figure 5. In principle, VBC monomer grafting can occur in both the core and shell of the PE/PP fibres, as suggested by the high GY% obtained. However, the shell is expected to be more susceptible to graft polymerisation due to the direct exposure of its active surface to monomer diffusion during the reaction. To gain further insights into the localisation of grafting within the fibre components, the composition of the grafted

substrates was further examined under different grafting conditions in emulsion- and solvent-mediated grafting in relation to GY%.

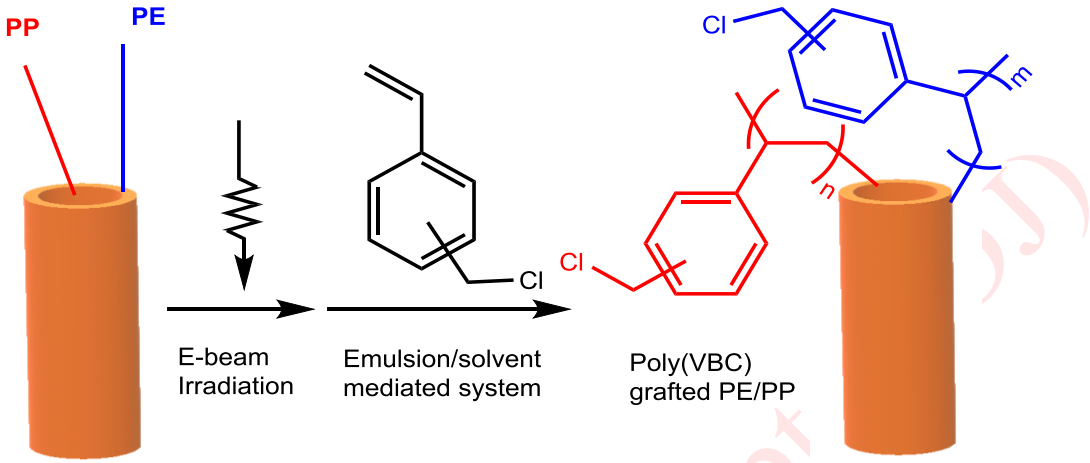

Figure 5. Schematic representation of the grafting of VBC on bi-component PE-PP fibres.

Elemental analysis of original PE/PP fibres and poly(VBC) grafted samples in relation to GY% was performed, and the obtained data are presented in Table 1. The percentage of C and H was reduced upon increasing GY, and this trend can be ascribed to the incorporation of poly(VBC) segments onto the PE/PP fibres. Poly(VBC) introduces chlorine atoms into the polymer matrix, thereby lowering the relative atomic fractions of C and H compared to the original PE/PP backbone. This compositional variation further confirms the successful grafting of VBC and is in good agreement with the gravimetric measurements.

Table 1. Elemental analysis of original PE/PP fibres and poly(VBC) grafted samples in relation to GY%.

Samples	Grafting Yield (%)	Elemental composition (%)			
		C	H	N	S
PE/PP fibres	-	86.84	12.91	<0.1	<0.05
PE/PP-*g*-poly(VBC)	40	82.23	11.57	<0.1	<0.05
PE/PP-*g*-poly(VBC)	80	78.32	9.46	<0.1	<0.05
PE/PP-*g*-poly(VBC)	150	70.60	8.30	<0.1	<0.05

Structural changes

X-ray diffraction analysis was carried out to evaluate the structural changes of PE/PP fibres grafted with poly(VBC) with different GY%, and the diffractograms are presented in Figure 6(a). PE/PP fibre sheet was used as a control sample. As observed, four diffraction peaks of PP component at 2θ of 14.22°, 17.06°, 18.71° and 21.75° represent the crystalline lattices of 110, 040, 130, and 041,

respectively [33]. The characteristic crystalline peaks for PE shell were observed at 21.75° and 24.22°, which correspond to reflection planes of 110 and 200, respectively [34,35]. No new peak and significant shift in the crystalline peak position were observed. These results suggest that the diffraction curve of PE/PP grafted with poly(VBC) resembles the original bicomponent PE/PP, which is identical to the lattices of PE and PP. However, the peak intensities were significantly reduced with increasing GY%. The broadening of the peaks and reduction in the intensity of the crystalline phase are direct consequences of the incorporation of amorphous grafted chains.

Thermal properties changes

The thermal behaviour of original PE/PP fibres and PE/PP fibres grafted with poly(VBC) with different GY% was evaluated with DSC, and the thermograms are shown in Figure 6b. The Original PE/PP fibrous sheet was used as a control sample. The endothermic peak at 128.3 ^{o}C represents the T_m of PE at the sheath layer, whereas bimodal endothermic peaks at 152.8 ^{o}C and 162.7 ^{o}C represent the T_m of PP. The sharpness of the peaks corresponding to PE at the sheath layers indicates the presence of crystalline regions in the fibres. This was coupled with the decrease in peak intensity upon increasing GY%. Interestingly, T_m of PE at 128.3 ^{o}C was not affected by increasing GY%, indicating that the original crystallites of PE found in the outer zone remained intact. This suggests that the grafting took place in the amorphous region of PE. The sharpness of the double endothermic peaks corresponding to PP at the core layers of the bicomponent fibres could be attributed to the crystalline regions in the fibres. The incorporation of poly(VBC) caused the reduction in peak intensity and transformation of bimodal endothermic peaks to a single peak that was accompanied by a decrease in T_m from 162.7 ^{o}C (PE/PP fibre) to 153.6 ^{o}C for GY of 150%. This suggests that poly(VBC) is amorphous, and the apparent decrease in crystallinity is attributed to the dilution of the inherent crystallinity of PP resulting from growing chains of amorphous poly(VBC). The reduction in the T_m from 162.7 ^{o}C to 153.6 ^{o}C indicates that grafting of poly(VBC) forms an irregular structure in the non-crystalline region and disrupts the structure in the crystallinity region. These findings are in complete agreement with the XRD results discussed earlier.

Thermal stability changes

Figures 6c and 6b show TGA thermograms of original PE/PP fibres and poly(VBC) grafted fibres with different GY%. In poly(VBC) grafted PE/PP fibres, PE/PP showed a single-step degradation pattern in which thermal degradation occurred in the range of 270–470 ^{o}C (Figure 6c) with DTG peak recorded at 364.2 ^{o}C (Figure 6d). This result is an indication for the compatibility of that PE with PP. Upon grafting, two distinct weight loss steps were observed. The first step occurred in the range of 270–395 ^{o}C, was due to the degradation of grafted poly(VBC) side chains, whereas the second step in the range of 395–510 ^{o}C, was attributed to the degradation of PE/PP backbone.

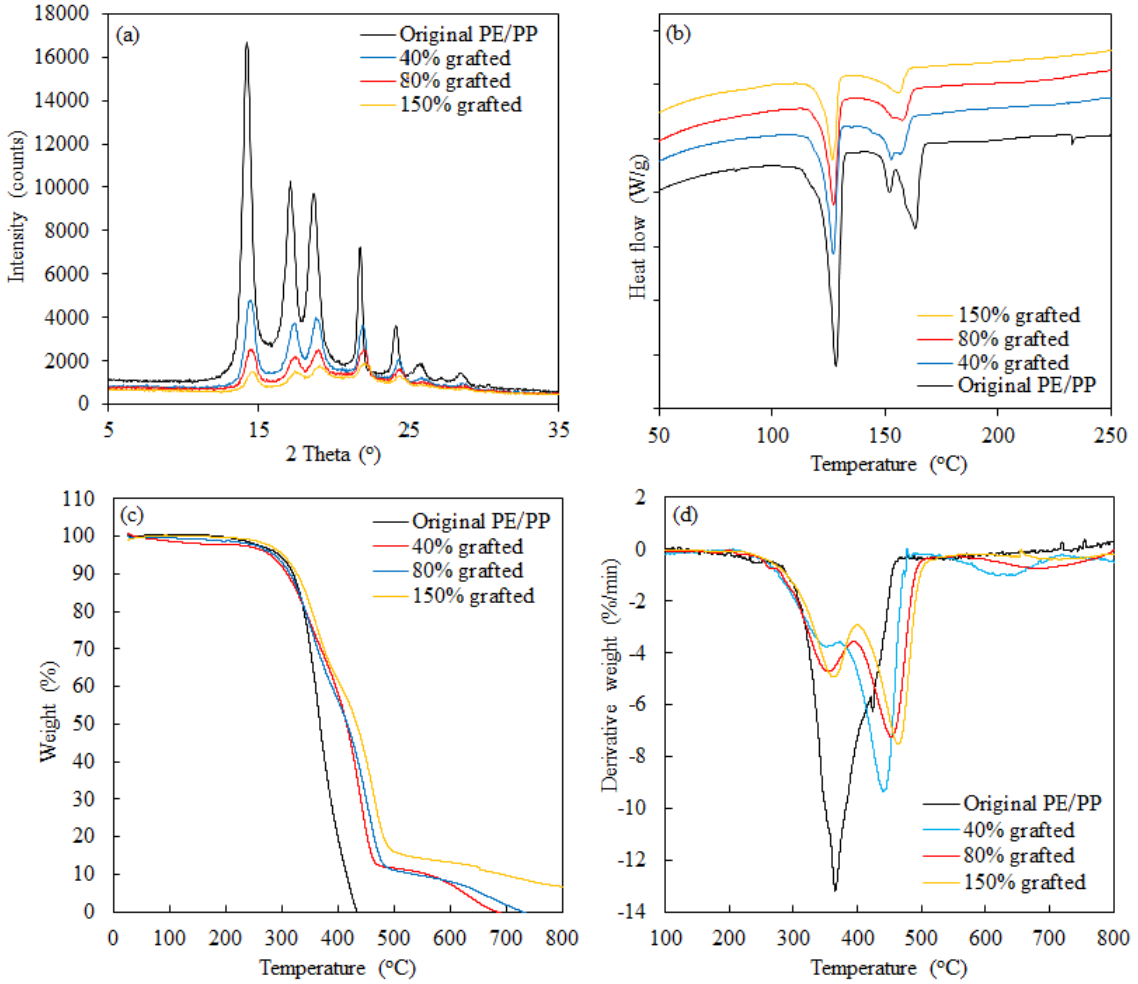

Figure 6. Structural and thermal analysis of original PE/PP fibres and poly(VBC) grafted samples with various GY%: (a) X-ray diffractograms, (b) DSC thermograms, (c) TGA thermograms and (d) DTG derivatives.

Morphological changes and EDX analysis

Figures 7 and 8 show FESEM images of the original PE/PP and VBC grafted PE-PP fibres with different GY% prepared using emulsion and solvent-mediated grafting. It can be observed that grafting of poly(VBC) induced distinct morphological modifications in the fibres, as proved by a progressive increase in surface roughness with increasing GY%. In solvent-mediated grafting, pronounced surface cracks were observed at a GY of 140%, which can be attributed to excessive swelling of the surface layers caused by methanol penetration during the grafting reaction. Such structural defects may compromise the mechanical stability of the fibres at high grafting levels. On the contrary, in the emulsion-mediated system, the fibres maintained their structural integrity even at a higher GY of 150%, indicating that the aqueous emulsion medium facilitates more uniform monomer diffusion and minimises solvent-induced damage to the fibre surface.

Further evidence on the grafting of poly(VBC) onto the PE/PP was obtained by Energy Dispersive X-ray analysis (EDX) mapping, and the images are presented in Figure 8 a &b. The images clearly reveal a uniform distribution of chlorine across the fibre surface and throughout the fibre cross-section,

indicating bulk grafting. This homogeneous incorporation of poly(VBC) within the fibrous substrate accounts for the uniform increase in fibre diameter as shown in Figure 9.

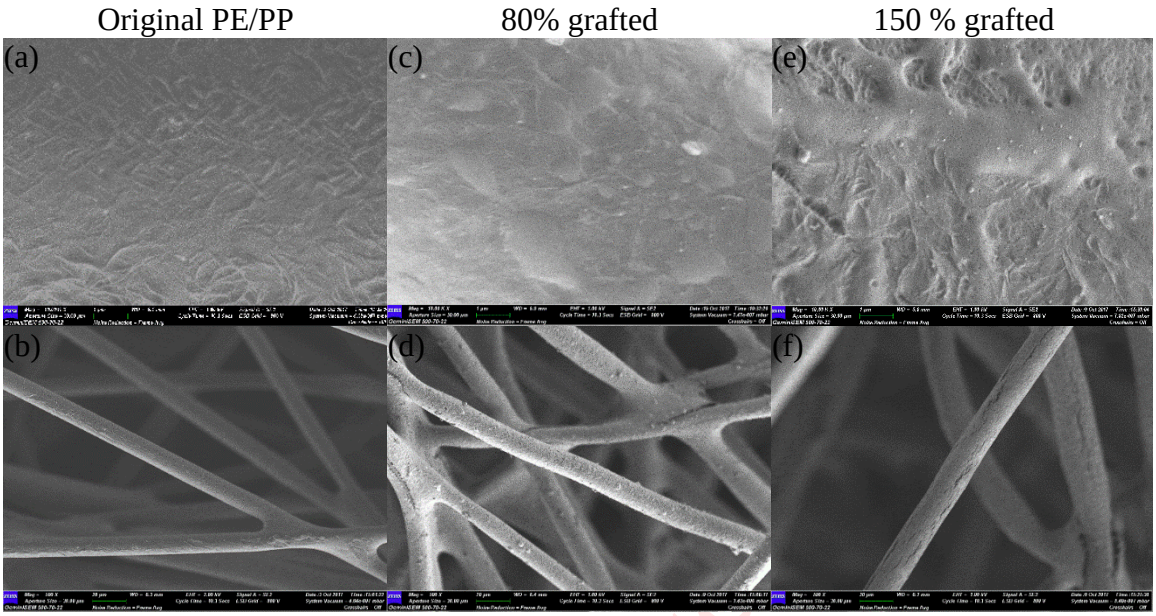

Figure 7. FESEM micrographs of: (a & b) original PE/PP, (c & d) 80% poly(VBC) grafted, and (e & f) 150% poly(VBC) grafted for surfaces and whole fibres modified using an emulsion grafting system.

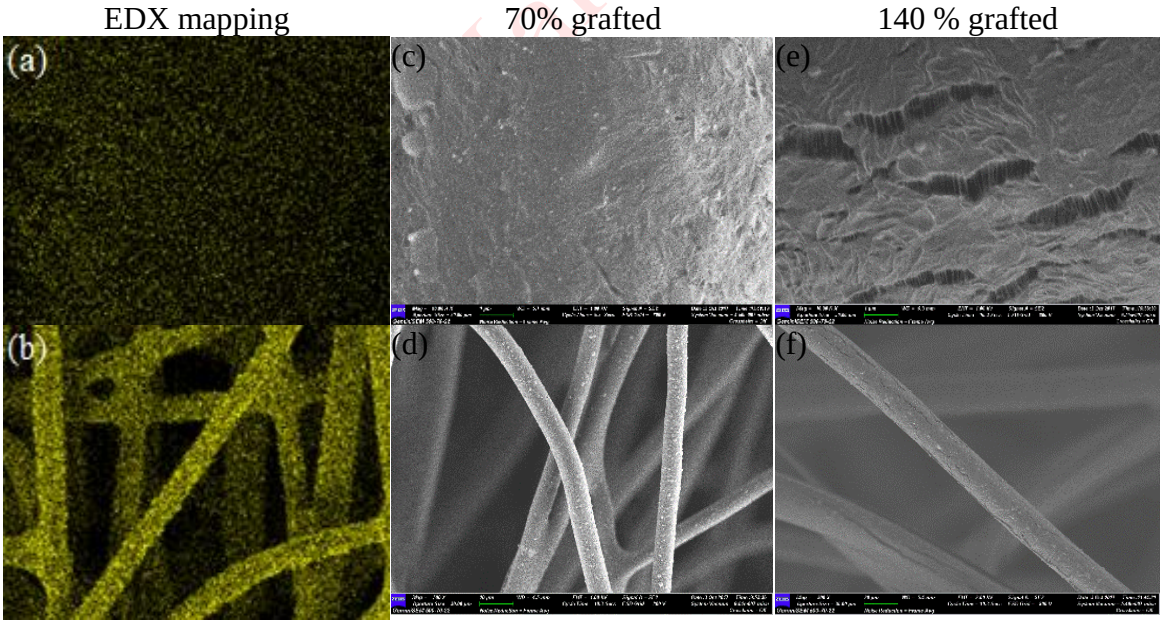

Figure 8. FESEM micrographs and corresponding EDX elemental mapping images for surfaces and whole fibres: (a & b) C1 mapping of 70 and 140 poly(VBC) grafted samples, (c & d) images of 70% poly(VBC) grafted samples and (e & f) 140% poly(VBC) grafted modified using solvent grafting system.

Figures 10 and 11 (a, b & c) show the cross-sectional FESEM images for the original PE/PP fibres and poly(VBC) grafted PE/PP fibres with different GY% obtained from emulsion- and solvent-

mediated grafting systems, respectively. In both grafting systems, the diameter and thickness of the PE and PP layers in the original bicomponent fibres increased after grafting, and the extent of this increase correlated with GY%. Specifically, higher grafting levels resulted in greater expansion of both component layers and overall fibre diameter. In contrast, Figure 10c reveals surface cracks in fibres prepared using the solvent-mediated grafting solution; however, no cracks were observed in the fibre cross-sections, indicating that the overall structural integrity was preserved.

The signal of chlorine (cps) and the average diameter of fibres (µm) from the line profiling of FESEM-EDX analysis in both grafting systems were found to increase with the increase in the GY%, as depicted from Figures 10d and 11d. The distribution of chlorine across the cross-sections of fibres prepared by both emulsion- and solvent-mediated grafting systems was found to parallel the increase in GY%.

In the emulsion-mediated system, the average diameters of fibres increased progressively from 12.2 µm at 40% GY to 13.8 µm at 80% GY and 17.5 µm at 150% GY. A similar trend was observed in the solvent-mediated system, with fibre diameters of 10.3, 15.2, and 18.9 µm corresponding to GY values of 28%, 70%, and 140%, respectively. The gradual and proportional increase in the fibre diameter with GY% confirms that VBC grafting occurred evenly and uniformly throughout the whole of PE/PP fibres, as reflected in the consistent morphological changes.

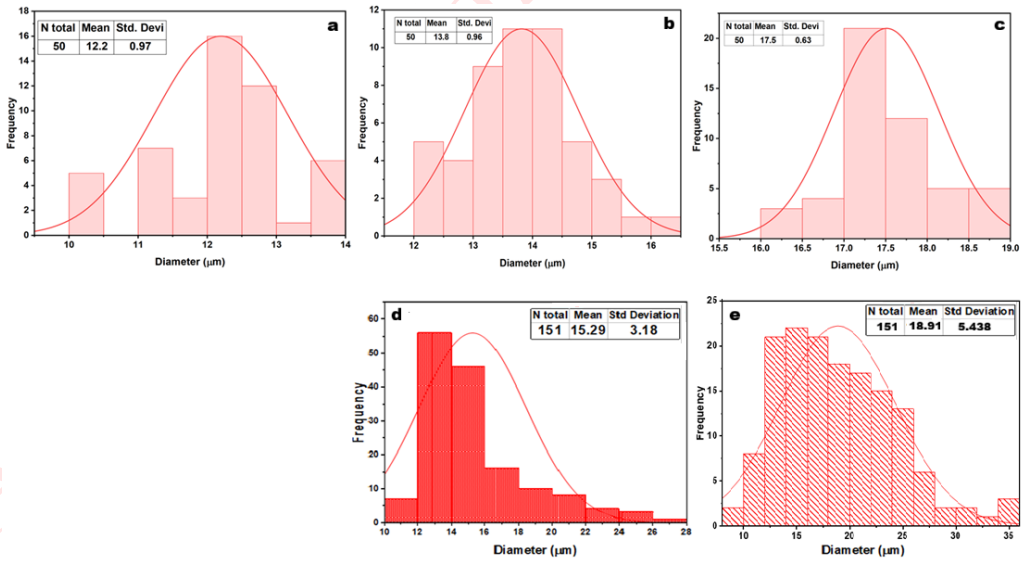

Figure 9. Average fibre diameter: (a) of original PE/PP fibres and poly(VBC) grafted fibres from emulsion grafting with GY of (b) 80% and (c) 150% and counterparts (d) and (e) from solvent grafting.

The density of chlorine in the sheath layer was significantly higher than the density of chlorine in the core layer in the grafted fibres prepared by emulsion-mediated grafting solution, whereas the density of chlorine in the core layer was slightly higher than the density of chlorine in the sheath layer in grafted fibres prepared by solvent-mediated grafting solution (Figures 10d and 11d). Even though the inherent

difference in the reactivity of radicals generated on PP and PE fibres during irradiation and subsequent grafting reaction will also play a role in the graft propagation behaviour [36]. This trend could also be ascribed to the enhanced diffusion rate of VBC onto the core layer when methanol was used as a solvent. Despite the bicomponent structure, in which a PE sheath surrounds and protects the PP core, radiation-induced radical initiation and subsequent monomer diffusion into the core layer prevailed in a way that led to bulk grafting.

These observations are in good agreement with the EDX mapping presented in Figure 11a, which clearly shows a uniform distribution of chlorine across the cross-section of the bicomponent PE/PP fibres. This uniformity indicates that poly(VBC) was successfully incorporated into both the PE sheath and the PP core. The generation of radicals in both layers during irradiation enabled RIG of VBC to proceed throughout the fibres, leading to bulk incorporation of poly(VBC) with consistent GY% and homogeneous distribution across the entire structure.

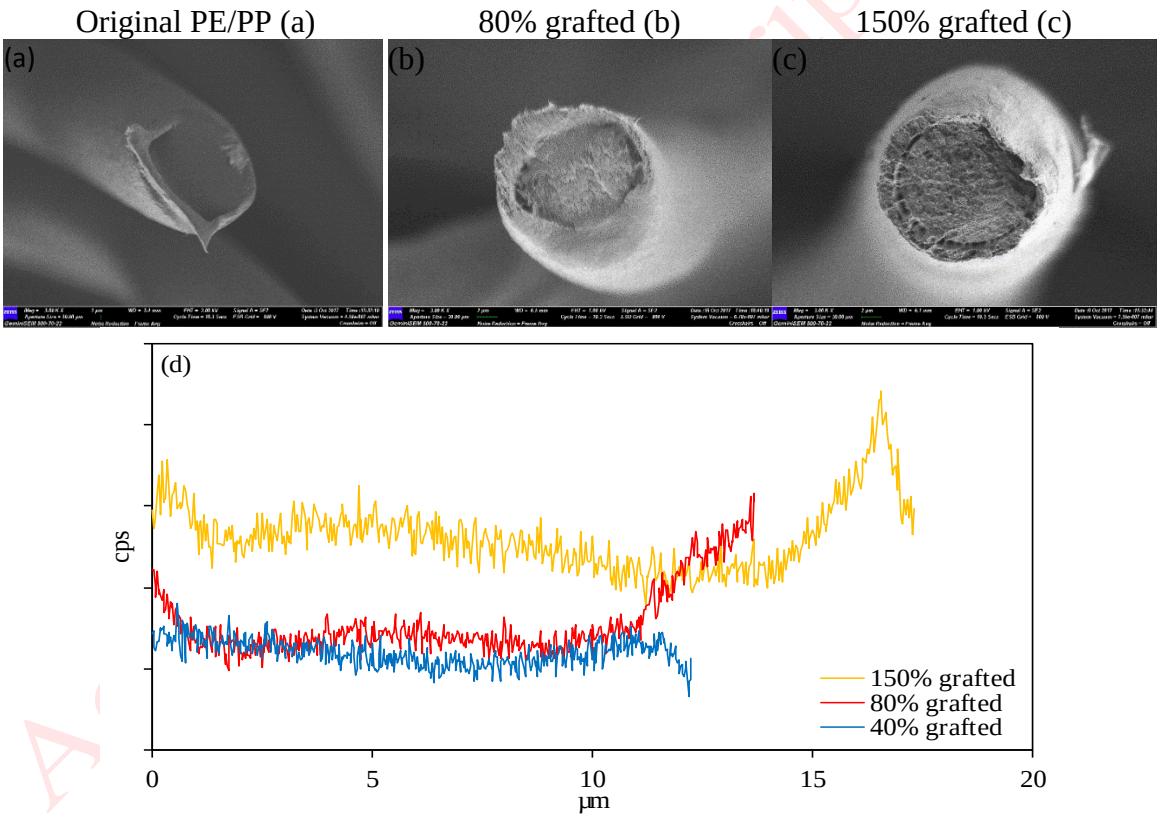

Figure 10. FESEM micrographs of: (a) original PE/PP, (b) 80% poly(VBC) grafted, and (c) 150% poly(VBC) grafted fibrous substrates, together with (d) FESEM EDX analysis of Cl profiling for fibres cross-sectional modified using emulsion grafting system.

The present results further indicate that VBC grafting onto PE/PP sheets is dictated by the fibrous morphology and sheath-core architecture, with grafting occurring on both the PE sheath and PP core due to radical generation in both layers during irradiation. This enables VBC to diffuse throughout the fibres, resulting in bulk incorporation of poly(VBC) characterised by consistent grafting yield and

homogeneous distribution across the entire nonwoven structure. The accumulation of grafted poly(VBC) on individual fibres leads to fibre thickening, which reduces the inter-fibre spacing and consequently decreases the overall porosity of the nonwoven sheet. This differs from RIGC of GMA onto porous films, which is governed by monomer diffusion within radicals' rich matrix pore network, with graft initiation occurring at the pore walls and propagation proceeding inward toward the pore interior, accompanied by polymer root formation invading PE matrix [16].

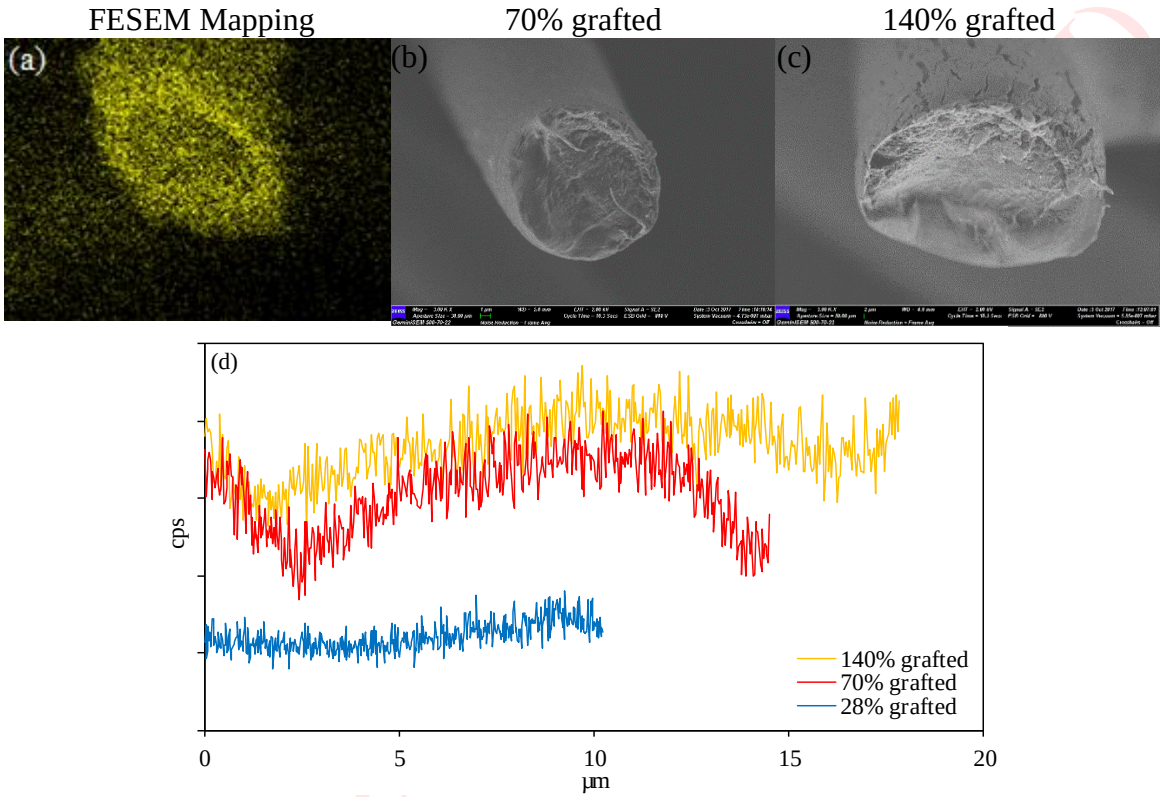

Figure 11. FESEM micrographs of: (a) 70% poly(VBC) grafted with EDX mapping images of Cl, (b) 70% poly(VBC) grafted, and (c) 140% poly(VBC) grafted fibrous substrates together with (d) FESEM EDX analysis of Cl profiling for fibre cross-sectional modified using a solvent grafting system.

Hydrophobicity of the grafted substrate

Figure 12 shows a representative shape of a water droplet on the bicomponent PE/PP fibrous sheets grafted with poly(VBC) at different GY%. The contact angle on the original (un-grafted) PE/PP surface was 0°, indicating complete water penetration into the fibrous sheet. After grafting with poly(VBC), the surface character changed from hydrophilic ($\alpha < 90°$) to hydrophobic ($\alpha > 90°$). The contact angle increased with increasing GY%, rising sharply to 130° at 40% GY and then gradually approaching a plateau, reaching 146° at 150% GY. This value is close to the threshold reported for superhydrophobic surfaces (>150°) [37]. It is worth noting that the measured contact angles on nonwoven fabrics reflect apparent wettability, influenced by both individual fibre properties and the fabric's mesh structure, including inter-fibre spacing and overall architecture. The porosity affects liquid spreading, droplet

penetration, and contact line stability, contributing to the observed values. Since all samples share identical structures, relative changes in contact angle mainly result from grafting-induced surface modification. Thus, the present results demonstrate that grafting poly(VBC) onto bicomponent PE/PP fibres provides an effective means of tuning surface wettability, converting the material from fully hydrophilic to highly hydrophobic, with higher GY% leading to near-superhydrophobic behaviour.

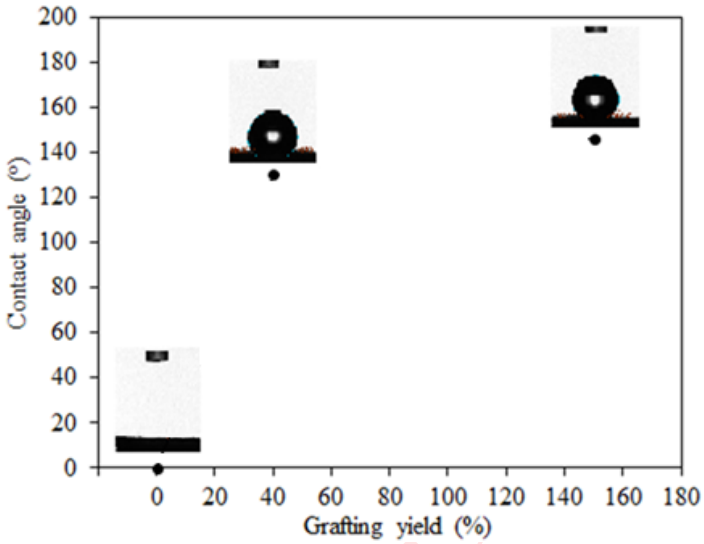

Figure 12. Representative of water contact angle of pristine PE/PP and corresponding grafted substrates.

Benefits of present study and potential applications of poly(VBC) grafted substrates

The poly(VBC)-grafted PE/PP fibres prepared in this study can serve as versatile precursors for further functionalization toward a wide range of applications. The benzylic chloride ($–CH_2$ –Cl) pendant groups incorporated in the structure provide reactive sites that can be readily transformed into ion-exchangeable functionalities such as quaternary ammonium salt, sulfonate, or phosphonate groups. RIG of VBC enables the controlled introduction of poly(VBC) side chains onto diverse polymer substrates of various physical forms (e.g., fibres, films, mats, and powders), with precise tuning of grafting density, distribution, and functionalization. Importantly, tailoring grafting parameters makes it possible to direct the incorporation of poly(VBC) chains from the surface to the bulk of the polymer matrix, thereby accommodating structure/morphology requirements of specific applications. For instance, post-grafting amination reactions with tailored functional groups can yield highly efficient adsorbents for the removal of pollutants from aqueous environments [38].

Particularly, adsorbents for CO_2 capture from flue gas and natural gas, which contain amine groups [25], and adsorbents for boron removal from industrial wastewater and produced waters, which contain glucamine groups [28], have strong potential for applications in environmental decontamination. Other potential applications of poly(VBC)-grafted fibrous sheets include the adsorption of oil-based pollutants from wastewater, facilitated by their intrinsic hydrophobic surface characteristics. Following functionalisation with quaternary ammonium hydroxide groups, these materials can also serve as

alkaline solid polymer catalysts for biodiesel production. Successful adoption of poly(VBC)-grafted fibrous sheets in such applications and other adsorption applications, however, implies the need for optimisation of a combination of properties, including ion-exchange capacity, porosity, and mechanical integrity to ensure both efficiency and long-term stability.

Other applications, including energy storage systems such as the use as separators in vanadium redox flow batteries (VRFBs), must simultaneously provide (i) high ionic conductivity while maintaining electrical insulation, (ii) excellent chemical and physical stability under strongly acidic conditions, and (iii) cost-effectiveness [39]. The use of polyolefin backbones such as PE/PP offers a cost advantage, and poly(VBC)-grafted PE/PP materials subjected to quaternization are promising candidates for such electrochemical applications. Particularly, studies that reported grafting of VBC onto substrates such as UHMWPE [40,41] with quaternary ammonium salt/poly(VBC) grafts demonstrated a strong potential for application in direct methanol fuel cell (DMFC). Other substrates, such as low-density PE [42], FEP [22,43], ETFE [44], and PEA films [22], which achieved bulk incorporation of quaternary ammonium salt functionalities throughout the polymeric substrate, which is a critical requirement for maximising ionic conductivity, showed promising application in the anion exchange membrane fuel cell (AEMFC). Cation exchange membranes containing sulfonic acid [22] and phosphonic acid [45] can be obtained by sulfonation and phosphonation of poly(VBC) substrates, respectively. A summary of potential applications of poly(VBC) grafted polyolefin substrates is presented in Table 2.

Table 2. Potential applications of poly(VBC) grafted fibrous sheets.

Chemical Modification	Functional group	Applications	Refs
Amination	Diethylenetriamine	Adsorbent for CO_2 Capture	[25]
Quaternization	Trimethylamine chloride	VRFB Separators	[39]
Quaternization	Trimethylammonium chloride	AEMFC membrane	[42]
Imidazolium treatment/alkalization	Imidazolium groups/OH-	AEMFC	[19]
Amination and cross-linking	Hexamethylenetetramine as an amination and cross-linking agent	AEMFC	[46]
Quaternization	Trimethylammonium hydroxide	DMFC	[41]
Quaternization	Guanidine derivative (1,1,3,3-tetramethyl-2-n-butylguanidine	DMFC	[40]
Base-catalysed hydrolysis for thiol formation, and oxidation with hydrogen peroxide	Sulfonic acid group	PEMFC	[22]
Phosphonation	Phosphonic acid group	N/A	(45)
Gulcamine treatment	*N*-methyl-*D*-glucamine	Adsorbent for boron removal	(28)
Amination/alkalization	Trimethylammonium hydroxide	Solid polymer basic catalyst for biodiesel	[47]
Quaternization	Quaternary ammonium chloride	Antimicrobial and mammalian cell selectivity	[48]

CONCLUSIONS

The grafting of VBC onto bicomponent PE/PP fibres was systematically examined under both emulsion- and solvent-mediated RIG conditions. The GY% exhibited a strong dependence on key reaction parameters, including monomer concentration, absorbed dose, and reaction temperature. Under equivalent conditions, the emulsion-based system consistently yielded higher GY% than the solvent-based system, achieving comparable grafting levels with approximately half the absorbed dose and monomer concentration. The superior efficiency of the emulsion system is attributed to enhanced radical stability and improved monomer diffusion within the aqueous emulsion medium. Diffusion of the VBC monomer through both the sheath and core enabled grafting onto the PE sheath and PP core of the fibres, indicating that modification occurred throughout the fibre bulk rather than being confined only to the surface. EDX mapping revealed preferential incorporation of poly(VBC) chains in the PE sheath compared to the PP core under emulsion-mediated grafting. Despite high grafting levels, the structural integrity of the PE/PP fibres was maintained, and the grafts were homogeneously distributed across the cross-section, confirming uniform radical accessibility. These results demonstrate that PE/PP-*g*-poly(VBC) prepared via emulsion RIG serves as a robust intermediate for subsequent post-grafting functionalization, enabling tailored properties for environmental and energy-related applications.

ACKNOWLEDGEMENTS

The authors would like to acknowledge the financial support of the Ministry of Higher Education (Malaysia) for funding this research under FRGS under grant no. FRGS/1/2018/TK05/MOSTI/03/1. The authors also wish to thank the Malaysia Nuclear Agency/Ministry of Science, Technology, and Innovation (MOSTI) for technical support.

CONFLICTS OF INTEREST

The authors have no conflicts of interest.

AUTHORS' CONTRIBUTIONS

Teo Ming Ting: Conceptualisation, supervision, funding acquisition, and preparation of the first draft. **Ebrahim Abouzari Lotf:** Conceptualisation, Investigation, data curation, and preparation of the first draft. **Mohamed Mahmoud Nasef:** Resources, writing-review and editing, and funding acquisition. **Wen Soong Lok:** Material synthesis and data curation.

Thye Foo Choo: Analysis and data curation. **Nur Athilah Kamarudin**: Material synthesis and data curation. **Ee Ling Aw**: Material synthesis and data curation. **Nur Ashikin Mohamed**: Visualisation and software.

REFERENCES

1. Russell SJ (2022) Handbook of nonwovens. 2nd edition. Cambridge: Woodhead publishing, (The Textile Institute book series).

2. Zhao R, Wadsworth LC, Sun C, Zhang D (2003) Properties of PP/PET bicomponent melt blown microfiber nonwovens after heat-treatment. Polymer International 52: 133-137 [CrossRef]

3. Farukh F, Demirci E, Sabuncuoglu B, Acar M, Pourdeyhimi B, Silberschmidt VV (2015) Mechanical analysis of bi-component-fibre nonwovens: Finite-element strategy. Composites Part B: Engineering 68: 327-335 [CrossRef]

4. Wang H, Jin X, Mao N, Russell SJ (2010) Differences in the tensile properties and failure mechanism of PP/PE core/sheath bicomponent and PP spunbond fabrics in uniaxial conditions. Textile Research Journal 80: 1759-1767 [CrossRef]

5. Lu L, Xing D, Xie Y, Teh KS, Zhang B, Chen S, Tang Y (2016) Electrical conductivity investigation of a nonwoven fabric composed of carbon fibers and polypropylene/polyethylene core/sheath bicomponent fibers. Materials & Design 112: 383-391 [CrossRef]

6. Chand S, Bhat GS, Spruiell JE, Malkan S (2001) Structure and properties of polypropylene fibers during thermal bonding. Thermochimica Acta 367-368: 155-160 [CrossRef]

7. Benkocká M, Lupínková S, Knapová T, Kolářová K, Matoušek J, Slepička P, Švorčík V, Kolská Z (2019) Antimicrobial and photophysical properties of chemically grafted ultra-high-molecular-weight polyethylene. Materials Science and Engineering: C 96: 479-486 [CrossRef]

8. Ting TM, Nasef MM, Sithambaranathan P (2017) Kinetic investigations of emulsion- and solvent-mediated radiation induced graft copolymerization of glycidyl methacrylate onto nylon-6 fibres. Journal of Radioanalytical and Nuclear Chemistry 311: 843-857 [CrossRef]

9. Kritzer P (2004) Separators for nickel metal hydride and nickel cadmium batteries designed to reduce self-discharge rates. Journal of Power Sources 137: 317-321 [CrossRef]

10. Kritzer P, Cook JA (2007) Nonwovens as Separators for Alkaline Batteries. Journal of The Electrochemical Society 154: A481 [CrossRef]

11. Ao J, Zhang H, Xu X, Yao F, Ma L, Zhang L, Ye B, Li Q, Xu L, Ma H (2019) A novel ion-imprinted amidoxime-functionalized UHMWPE fiber based on radiation-induced crosslinking for selective adsorption of uranium. RSC Advances 9: 28588-28597 [CrossRef]

12. Dietz TC, Tomaszewski CE, Tsinas Z, Poster D, Barkatt A, Adel-Hadadi M, Bateman FB, Cumberland LT, Schneider E, Gaskell K, LaVerne J, Al-Sheikhly M (2016) Uranium removal from seawater by means of polyamide 6 fibers directly grafted with diallyl oxalate through a single-step, solvent-free irradiation process. Industrial & Engineering Chemistry Research 55: 4179-4186 [CrossRef]

13. Kavaklı PA, Kavaklı C, Seko N, Tamada M, Güven O (2007) Radiation-induced grafting of dimethylaminoethylmethacrylate onto PE/PP nonwoven fabric. Nuclear Instruments and Methods in Physics Research Section B: Beam Interactions with Materials and Atoms 265: 204-207 [CrossRef]

14. Phu DV, Quoc LA, Duy NN, Hien NQ (2013) Study of incorporation of silver nanoparticles onto PE-g-PAAc nonwoven fabric by γ-irradiation for water treatment. Radiation Physics and Chemistry 88: 90-94 [CrossRef]

15. Seko N, Katakai A, Tamada M, Sugo T, Yoshii F (2004) Fine fibrous amidoxime adsorbent synthesized by grafting and uranium adsorption–elution cyclic test with seawater. Separation Science and Technology 39: 3753-3767 [CrossRef]

16. Ishihara R, Uchiyama S, Ikezawa H, Yamada S, Hirota H, Umeno D, Saito K (2013) Effect of dose on mole percentages of polymer brush and root grafted onto porous polyethylene sheet by radiation-induced graft polymerization. Industrial & Engineering Chemistry Research 52: 12582-12586 [CrossRef]

17. Rojek T, Gubler L, Nasef MM, Abouzari-Lotf E (2017) Polyvinylamine-containing adsorbent by radiation-induced grafting of N-Vinylformamide onto ultrahigh molecular weight polyethylene films and hydrolysis for CO_2 capture. Industrial & Engineering Chemistry Research 56: 5925-5934 [CrossRef]

18. Monthéard JP, Jegat C, Camps M (1999) Vinylbenzylchloride (chloromethylstyrene), Polymers, and copolymers. Recent reactions and applications. Journal of Macromolecular Science, Part C: Polymer Reviews 39: 135-174 [CrossRef]

19. Abouzari-Lotf E, Jacob MV, Ghassemi H, Zakeri M, Nasef MM, Abdolahi Y, Abbasi A, Ahmad A (2021) Highly conductive anion exchange membranes based on polymer networks containing imidazolium functionalised side chains. Scientific Reports 11: 3764 [CrossRef]

20. Abouzari-lotf E, Ghassemi H, Nasef MM, Ahmad A, Zakeri M, Ting TM, Abbasi A, Mehdipour-Ataei S (2017) Phase separated nanofibrous anion exchange membranes with polycationic side chains. Journal of Materials Chemistry A 5: 15326-15341 [CrossRef]

21. Cabalar PJE, Hamada T, Madrid JF, Seko N (2022) Synthesis of anion electrolyte membrane through radiation-induced graft polymerization of poly(4-vinylbenzyl chloride) onto isotactic polypropylene film. Mindanao Journal of Science and Technology 20: S1 [CrossRef]

22. Fei G, Sohn JY, Lee YS, Nho YC, Shin JH (2010) Preparation of poly(vinylbenzyl chloride)-grafted fluoropolymer films by using radiation grafting method. Polymer Korea 34: 464-468 [CrossRef]

23. Herman H, Slade RCT, Varcoe JR (2003) The radiation-grafting of vinylbenzyl chloride onto poly(hexafluoropropylene-co-tetrafluoroethylene) films with subsequent conversion to alkaline anion-exchange membranes: optimisation of the experimental conditions and characterisation. Journal of Membrane Science 218: 147-163 [CrossRef]

24. Hwang ML, Song JM, Ko BS, Sohn JY, Nho YC, Shin J (2012) Radiation-induced grafting of vinylbenzyl chloride onto a poly(ether ether ketone) film. Nuclear Instruments and Methods in Physics Research Section B: Beam Interactions with Materials and Atoms 281: 45-50 [CrossRef]

25. Mohamad NA, Nasef MM, Ali RR, Ahmad A, Abdullah TAT (2025) Evaluation of diethylenetriamine functionalized polymer adsorbent for carbon dioxide capture from natural gas. AIP Conf. Proc. 3113, 020017 [CrossRef]

26. Shin J, Fei G, Kang S, Ko B, Kang P, Nho YC (2009) Simultaneous radiation grafting of vinylbenzyl chloride onto poly(tetrafluoroethylene-co-hexafluoropropylene) films. Journal of Applied Polymer Science 113: 2858-2862 [CrossRef]

27. Ting TM, Nasef MM, Hashim K (2015) Modification of nylon-6 fibres by radiation-induced graft polymerisation of vinylbenzyl chloride. Radiation Physics and Chemistry 109: 54-62 [CrossRef]

28. Ting TM, Nasef MM, Hashim K (2015) Tuning N-methyl-d-glucamine density in a new radiation grafted poly(vinyl benzyl chloride)/nylon-6 fibrous boron-selective adsorbent using the response surface method. RSC Advances 5: 37869-37880 [CrossRef]

29. Aydinli B, Tinçer T (2001) Radiation grafting of various water-soluble monomers on ultra-high molecular weight polyethylene powder:. Radiation Physics and Chemistry 60: 237-243 [CrossRef]

30. Seko N, Bang LT, Tamada M (2007) Syntheses of amine-type adsorbents with emulsion graft polymerization of glycidyl methacrylate. Nuclear Instruments and Methods in Physics Research Section B: Beam Interactions with Materials and Atoms 265: 146-149 [CrossRef]

31. Vahdat A, Bahrami H, Ansari N, Ziaie F (2007) Radiation grafting of styrene onto polypropylene fibres by a 10MeV electron beam. Radiation Physics and Chemistry 76: 787-793 [CrossRef]

32. Nava-Ortiz C, Burillo G, Bucio E, Alvarez-Lorenzo C (2009) Modification of polyethylene films by radiation grafting of glycidyl methacrylate and immobilization of β-cyclodextrin. Radiation Physics and Chemistry 78: 19-24 [CrossRef]

33. Nishino T, Matsumoto T, Nakamae K (2000) Surface structure of isotactic polypropylene by X-ray diffraction. Polymer Engineering & Science 40: 336-343 [CrossRef]

34. Inci B, Wagener KB (2011) Decreasing the alkyl branch frequency in precision polyethylene: pushing the limits toward longer run lengths. Journal of the American Chemical Society 133: 11872-11875 [CrossRef]

35. Liao CZ, Tjong SC (2013) Mechanical and thermal performance of high-density polyethylene/alumina nanocomposites. Journal of Macromolecular Science, Part B 52: 812-825 [CrossRef]

36. Sherazi TA (2014) Radiation-induced grafting. In: Drioli, E., Giorno, L. (eds) Encyclopedia of Membranes. Springer, Berlin, Heidelberg [CrossRef]

37. Luzinov I (2007) Nanofabrication of thin polymer films. In: Nanofibers and nanotechnology in textiles, Brown PJ, Stevens K, editors (Eds), Cambridge, UK, Woodhead Publishing: 448–469

38. Wojnárovits L, Földváry CsM, Takács E (2010) Radiation-induced grafting of cellulose for adsorption of hazardous water pollutants: A review. Radiation Physics and Chemistry 79: 848-862 [CrossRef]

39. Abdiani M, Abouzari-Lotf E, Ting TM, Moozarm Nia P, Sha'rani SS, Shockravi A, Ahmad A (2019) Novel polyolefin based alkaline polymer electrolyte membrane for vanadium redox flow batteries. Journal of Power Sources 424: 245-253 [CrossRef]

40. Sherazi TA, Zahoor S, Raza R, Shaikh AJ, Naqvi SAR, Abbas G, Khan Y, Li S (2015) Guanidine functionalized radiation induced grafted anion-exchange membranes for solid alkaline fuel cells. International Journal of Hydrogen Energy 40: 786-796 [CrossRef]

41. Sherazi TA, Yong Sohn J, Moo Lee Y, Guiver MD (2013) Polyethylene-based radiation grafted anion-exchange membranes for alkaline fuel cells. Journal of Membrane Science 441: 148-157 [CrossRef]

42. Wang L, Brink JJ, Liu Y, Herring AM, Ponce-González J, Whelligan DK, Varcoe JR (2017) Non-fluorinated pre-irradiation-grafted (peroxidated) LDPE-based anion-exchange membranes with high performance and stability. Energy & Environmental Science 10: 2154-2167 [CrossRef]

43. Slade R, Varcoe J (2005) Investigations of conductivity in FEP-based radiation-grafted alkaline anion-exchange membranes. Solid State Ionics 176: 585-597 [CrossRef]

44. Ko B, Sohn J, Shin J (2012) Radiation-induced synthesis of solid alkaline exchange membranes with quaternized 1,4-diazabicyclo[2,2,2] octane pendant groups for fuel cell application. Polymer 53: 4652-4661 [CrossRef]

45. Schmidt-Naake G, Böhme M, Cabrera A (2005) Synthesis of proton exchange membranes with pendent phosphonic acid groups by irradiation grafting of VBC. Chemical Engineering & Technology 28: 720-724 [CrossRef]

46. Vengatesan S, Santhi S, Sozhan G, Ravichandran S, Davidson DJ, Vasudevan S (2015) Novel cross-linked anion exchange membrane based on hexaminium functionalized poly(vinylbenzyl chloride). RSC Advances 5: 27365-27371 [CrossRef]

47. Nasef MM, Ting TM, Abbasi A, Layeghi-moghaddam A, Alinezhad S, Hashim K (2016) Radiation grafted adsorbents for newly emerging environmental applications. Radiation Physics and Chemistry 118: 55-60 [CrossRef]

48. Rusli W, Halleluyah PM, Jun LX, Lakshminarayanan R, Parthiban A (2023) Synthesis, characterization and cell selectivity of poly(quaternary ammonium chlorides): effect of the degree of quaternization and copolymer composition. Materials Advances 4: 4954-4964 [CrossRef]